Design and Development of a Fluid Immersion Cooled, SiC MOSFET, 37.5 kW, Bi-Directional Motor Converter

Susanah Kowalewski*, Rebecca Buehrle†, Matthew Faykus‡, John Maroli§, and Matthew Granger¶
NASA Glenn Research Center, Cleveland, OH, 44135

NASA's SUb-sonic Single Aft eNgine (SUSAN) aircraft is a concept aircraft whose architecture is that of a subsonic regional jet transport aircraft. SUSAN contains a single turbofan engine coupled to an electrified aircraft propulsion (EAP) system. To provide a path towards this goal, a 25% scale version of the SUSAN aircraft is being researched. A main component of the 25% power train is the Motor And Generator Intelligent Converter (MAGIC). This paper presents the design, development, and initial test results from MAGIC, a 37.5 kW, fluid immersion cooled, silicon carbide (SiC) MOSFET-based, bi-directional converter and controller.

I. Introduction

MAGIC was designed as part of an EAP architecture which includes an internal combustion engine (ICE), a 150 kW generator, a distributed electric propulsion (DEP) system, and tail engine. The architecture is shown in Figure 1. The ICE is connected to the 150 kW generator which outputs four sets of three-phase AC connections. Each of these sets is connected to a MAGIC operating at 37.5 kW. MAGIC then distributes a 270 V nominal DC bus throughout the aircraft to power both the wing and tail engines. In the tail engine, up to two more MAGICs could be connected to motors to provide thrust for the aircraft. Because of the dual application potential for MAGIC, it is required to be a bi-directional converter, capable of converting DC to AC and AC to DC. The term 'converter' as used in this paper shall be taken to mean both the high-power electronics and the motor controller circuitry, as they are designed together in one unit. Its power level requirements are 37.5 kW, a quarter of 150 kW, and 270 V DC. The converter will be located in the fuselage of the aircraft and will not have access to air flow for cooling. This presented the thermal challenge of cooling MAGIC without airflow and without adding an entire separate cooling system. The decision was then made to create a fluid immersion cooled converter, tying in with the rest of the aircraft's cooling system.

*MAGIC Lead, Power - Diagnostics and Electromagnetics, NASA GRC
†MAGIC Mechanical Engineer, Materials and Structures - Mechanical Systems Design and Integration, NASA GRC
‡MAGIC Thermal Engineer, Propulsion - Thermal Systems and Transport Processes, NASA GRC
§MAGIC Software Lead, Systems - Flight Software, NASA GRC
¶AATT Task Lead, Power - Power Management and Distribution, NASA GRC

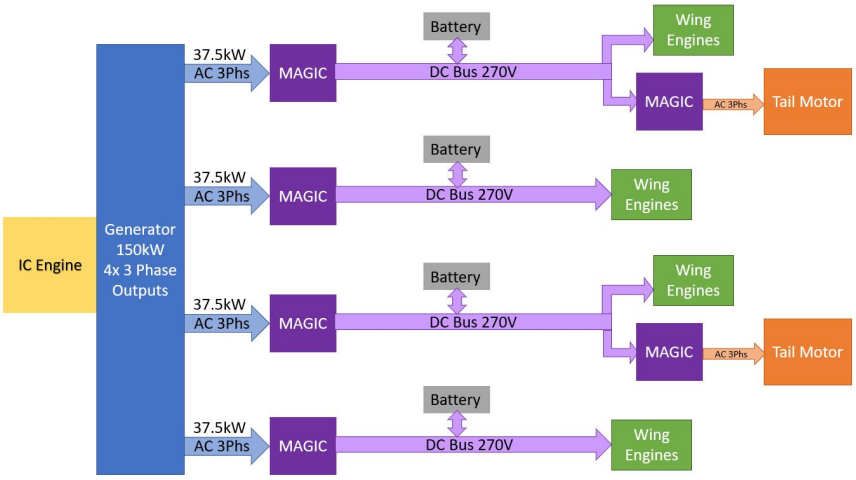

Fig. 1 SUSAN 25% Scale Aircraft Block Diagram

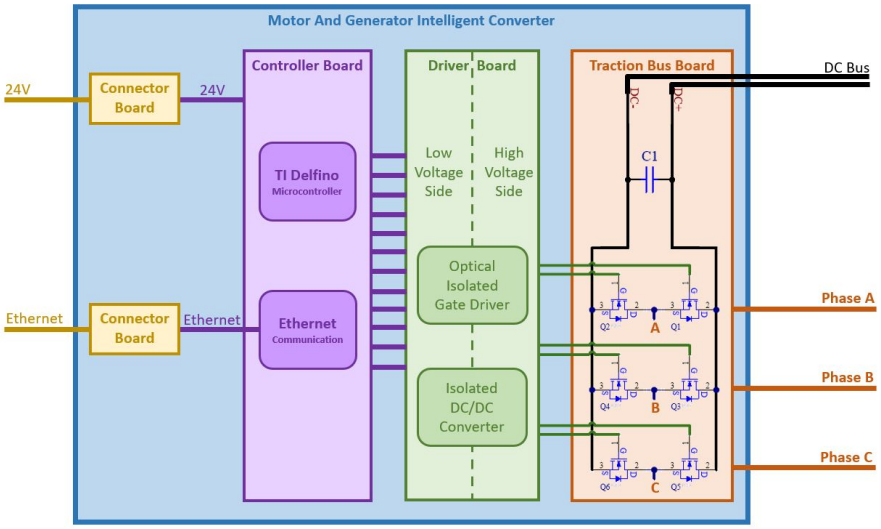

Fig. 2 MAGIC Block Diagram

The converter design has heritage from the NASA X-57 Maxwell project's converters, both the High Lift Motor Controller (HLMC) and Cruise Motor Controller (CMC). The controller circuitry foundation evolved from HLMC, as HLMC was developed at NASA Glenn Research Center (GRC), and is compatible with the custom software and graphical user interface (GUI) which were designed for HLMC, with minor updates. The power stage circuitry foundation evolved from CMC, due to the similar power level requirements.

Immersion cooling the converter offers several advantages. First, as mentioned previously, by using immersion cooling the converter does not require access to direct airflow and can therefore be placed anywhere on the aircraft. Previously developed motor converters, such as HLMC and CMC, required access to airflow for cooling. In addition, this system does not require bulky external heat sinks, which would typically be cooled by an air stream. Immersion cooling is also able to cool all electronics simultaneously, whereas a traditional heatsink method only cools the hottest parts. This also helps to keep parts within their temperature limits, as some of the lower power electronics tend to have lower temperature limits, such as 85 °C. By cooling all these parts instead of just the biggest power loss parts, the entire system can be kept at lower temperature, leading to longer run time capabilities. This constant thermal management could also potentially lead to longer life of the parts and increase the efficiency of the converter by keeping all components closer to their optimal operating temperature.

II. Electrical Design

A. Electrical Architecture

The converter topology is a three-phase, six switch converter, capable of bi-directional operation converting DC to AC or AC to DC. This is a "sensorless" system, in that it does not utilize an encoder or other motor position feedback device. The converter is divided into three main circuit boards and two auxiliary boards. There is a Controller Board, Driver Board, Traction Board, and two auxiliary Connector Boards to interface to the box-mounted hermetic connectors. The Controller Board interfaces the low voltage electronics through the Connector Boards out of the box, including the 24 V avionics bus and Ethernet communications signals. The Traction Board interfaces the high voltage electronics out of the box including the 270 V DC bus and three-phase AC signals. The Driver Board is the internal interface between the low voltage and high voltage components. A block diagram of this configuration can be seen in Figure 2.

B. Controller Board

The Controller Board contains many low voltage circuits. It operates the software and controls the MOSFET switching of the Driver Board. The top and bottom of the Controller Board are shown in Figure 3 . It contains isolated

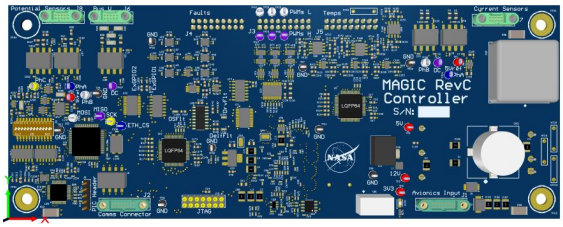

(a) MAGIC Controller Board Top Side

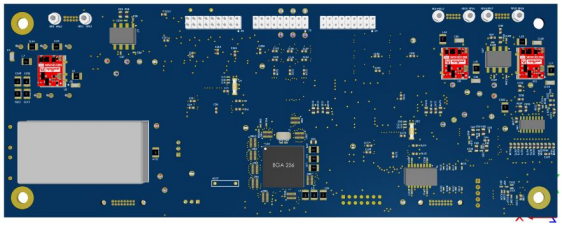

(b) MAGIC Controller Board Bottom Side

Fig. 3 MAGIC Controller Board

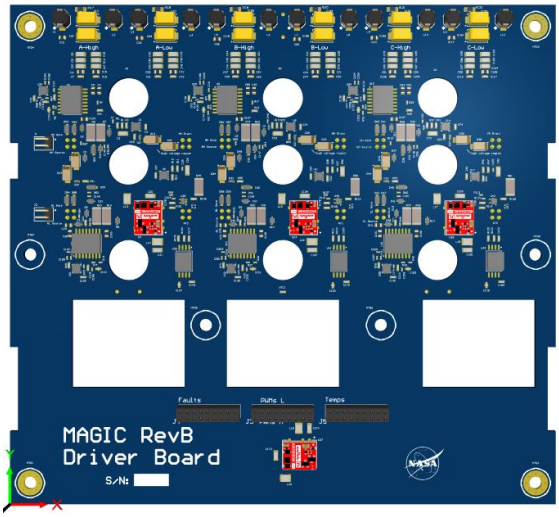

(a) MAGIC Driver Board Top Side

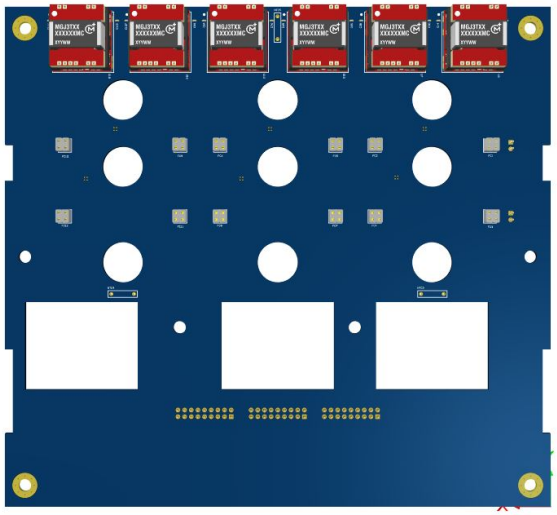

(b) MAGIC Driver Board Bottom Side

Fig. 4 MAGIC Driver Board

phase and bus current and voltage sensors, fault circuitry, and temperature sensor interfaces. These isolated components are placed in isolated regions which are critical for minimizing noise. The isolation is not limited to the components; it is designed into the circuit board by having no-copper regions at these boundaries on all layers of the PCB. A TI Delfino microcontroller is used for control; it interfaces with two ADCs to read all the sensor signals, and with PIC and PHY ICs for Ethernet communication. This board also contains three chassis-bonded mounting holes that capacitively couple several signals to the chassis to reduce noise. Bypass capacitors between the mounting holes and control board signals improve noise immunity by providing a low impedance path for common mode noise currents back to the power stage through chassis and away from the controller signals. Additionally, sensitive signals, such as fault lines, were run as differential signals and increased from 3.3 V up to 5 V where possible to add robustness.

C. Driver Board

The Driver Board provides the interface between the low voltage and high voltage components. The top and bottom of the Driver Board are shown in Figure 4. It contains the isolated gate drive ICs, isolated DC/DC power supplies, and overcurrent fault detection. The isolated components are again placed across isolated PCB areas of no-copper; additionally, these components must have extremely small coupling capacitance to minimize noise coupling from the high side to the low side. The overcurrent protection is a standard desaturation circuit. The Driver Board also contains the low power connections for the SiC MOSFET modules which were used; these plug into the bottom of the board, and the circular holes in the board allow for the high power bus bar connections to pass through. This board also contains four plated mounting holes that capacitively couple several signals to the chassis for noise immunity as described on the Controller Board.

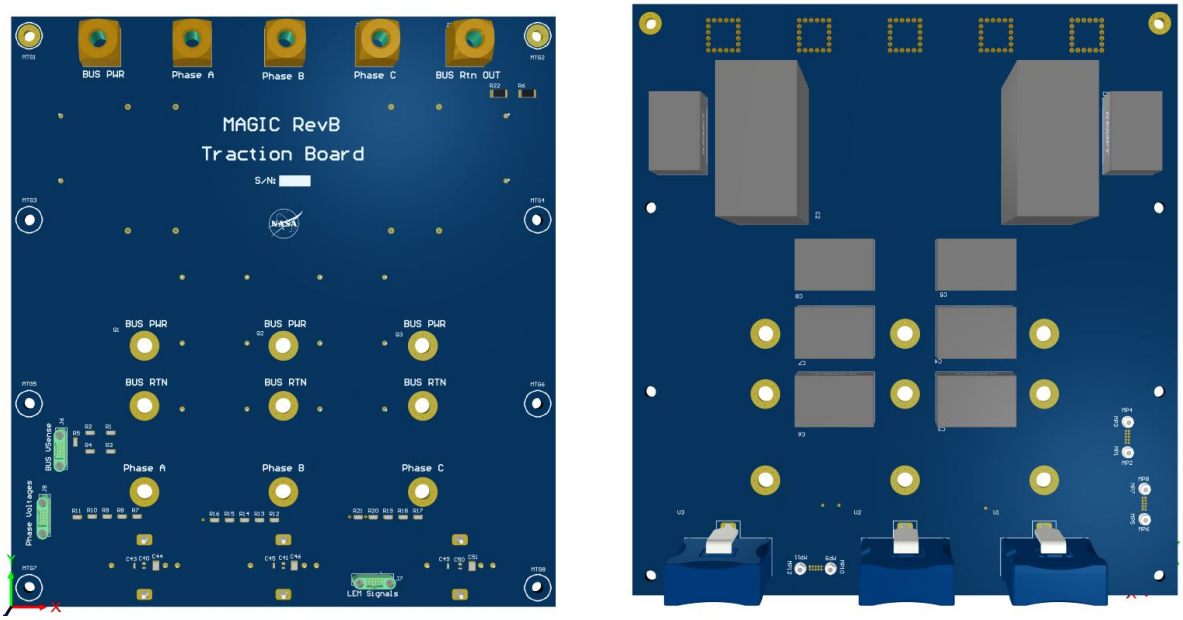

(a) MAGIC Traction Board Top Side **(b) MAGIC Traction Board Bottom Side**

Fig. 5 MAGIC Traction Board

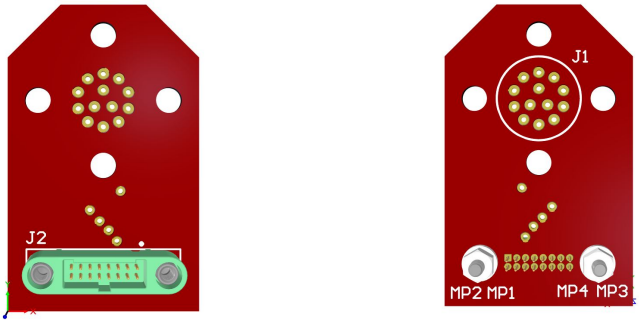

(a) MAGIC Connector Board Top Side **(b) MAGIC Connector Board Bottom Side**

Fig. 6 MAGIC Connector Board

D. Traction Board

The Traction Board contains the connections for the high power signals for the MOSFETs and connections out of the box for the three phase AC and DC bus power. The top and bottom of the Traction Board are shown in Figure 5. It also contains DC filter capacitors and the capacitor part of an LC filter aimed at reducing common mode EMI in the DC bus. The capacitors are coupled to the chassis via the plated standoffs on the one end of the PCB. The inductor part of the filter sits underneath the Traction Board with the DC bus wires running through it, before landing on the Traction Board. By terminating this LC filter to the chassis, the goal is to keep the current loop small and contained within the converter to prevent EMI from exiting the system via the DC lines. Additionally, this board contains the source of the phase and bus current and voltage sensor readings.

E. Connector Board

The Connector Boards, seen in Figure 6, contain the connections for the low voltage avionics power and communications signals. There are two Connector Boards, each soldered into a hermetic connector to pass out of the box. A short cable is run from each Connector Board, to land on the Controller Board.

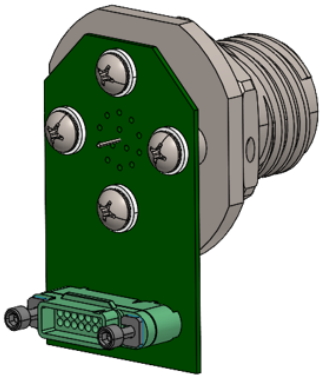

Fig. 7 Hermetic Connector attached to Connector Board

III. Mechanical and Thermal Design

The mechanical design took inspiration from the X-57 CMC enclosure, and updated and adapted it for this immersion cooled application. The box was modeled in CAD software with 3D models of the circuit boards to ensure proper alignment and fit of all parts.

A. Fluid

The fluid in the system is polyalphaolefin (PAO), specifically Opticool-MIL 87252, which is a dielectric fluid. Initially, non-dielectric fluids were researched, as they possessed slightly better thermal characteristics. However, it was determined that the coating technology for PCBs and other surfaces, which would be required for a non-dielectric fluid, was not suitable for this application. PAO was chosen for its dielectric properties and because it can already be found in use on some military aircraft. It is also compatible with a wide range of materials. There are many temperature sensors located throughout the design to monitor both the fluid and electronics temperatures.

B. External Enclosure Connectors

There are three different external connectors in the enclosure; one kind for the low voltage avionics power and communication, another for the DC bus and fluid connection, and the last for the AC phase connections. There are two low voltage connectors, one for the avionics power and one for communication. These connectors are glass sealed hermetic connectors with a Viton o-ring. The o-ring material type was chosen as it demonstrated the most resilience when exposed to PAO. These hermetic connectors are soldered into the Connector Boards, seen in Figure 7, which then use board-to-board cable connectors to take signals to the Controller Board. The hermetic connectors with the Connector Boards are then installed into the enclosure, as seen in Figure 8.

The combination DC bus and fluid connectors were a unique design developed at NASA GRC and were previously used on the HiACT project [1]. These connectors combine the DC bus and cooling fluid into one, with DC+ paired with fluid inlet and DC- with the fluid outlet. This combination of DC power and fluid is potentially very advantageous for electrified aircraft. By actively cooling the copper carrying the DC power, much more current can be carried on less copper than traditional wires, which are not actively cooled. This leads to a reduction in the necessary amount of copper for the aircraft, therefore reducing the weight of the plane, which in turn boosts the "fuel economy".

The connector itself is a copper tube that passes through a plastic NPT tube fitting, seen in Figure 9a. The copper passes directly to the interior of the enclosure, carrying the DC signal, while the hollow aspect of the tube passes the fluid. Once inside the box, the DC signals are taken off the tubes using cables made in house, with wire which was selected for its chemical resistance and flexibility to maneuver around obstacles in the enclosure. Notably, these wires had to pass through an inductor located in the middle of the enclosure, this inductor was part of the built-in LC common mode filter discussed in the electrical section, before landing on the Traction Board. Outside the box, the electrical and fluid lines were split off with the fluid going to a heater/chiller pump and the electrical connections using a clamp to go to a DC load or supply depending on the test setup.

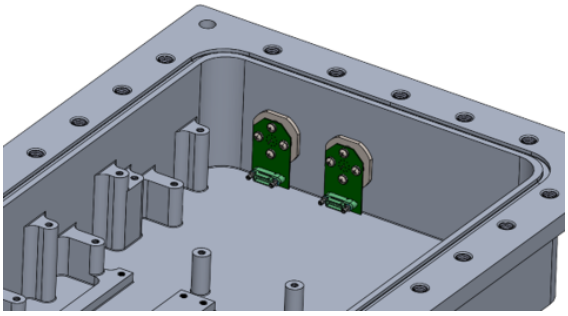

(a) Hermetic Connectors and Connector Board Inside Enclosure

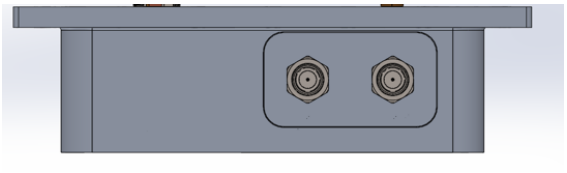

(b) Hermetic Connectors from Outside the Enclosure

Fig. 8 Hermetic Connectors Installed in Enclosure

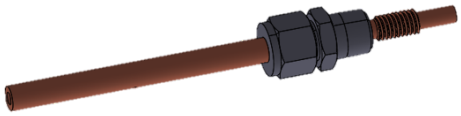

(a) Hollow DC Bus Tube and Plastic Fitting

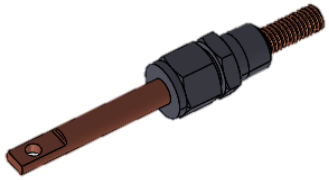

(b) Solid AC Rod and Plastic Fitting

Fig. 9 High Power Connectors

The AC phase connectors were modeled off the DC connectors, but used copper rods instead of tubes, as the fluid was not passed through these, seen in Figure 9b. On the inside of the enclosure, cables were again used to connect from the rods to the Traction Board. Outside the box, the AC rods had a hole on the end to connect to a standard wire with a ring terminal.

These power connectors can be seen installed in the box in Figure 10. The DC tubes are the two outside connectors, while the three AC connectors are the rods in the middle. The DC+ / fluid inlet connector is physically raised higher in the box to allow the fluid to enter the enclosure at the top, move over the lower power electronics, and then exit via the bottom DC- / fluid outlet connector.

C. MOSFETs, Heat Sinks, and Manifold

The base of the design is the MOSFET modules; these components have the greatest heat output, with the most power loss, and also require close physical proximity to their driver circuits. The MOSFET loss varies with the switching frequency. Analysis shows a 40 kHz switching frequency corresponds to 330 W of loss in each MOSFET module, which contains two MOSFETs, at full power. An 80 kHz switching frequency corresponds to 380 W of loss in each module. MAGIC can handle both cases. To effectively cool the MOSFETs, copper elliptical pin fin heat sinks were designed to mount to the bottom of the MOSFETs, seen in Figure 11. This increases the surface area of the FETs, allowing for the necessary heat dissipation. A special thermal epoxy was used to bond the heat sinks to FETs which would maintain adequate thermal conduction, hold the heat sinks in place, and not negatively interact with the PAO fluid. The MOSFETs with their small pin fin heat sinks were placed on rails on the bottom of the enclosure and screwed into place, seen in Figure 12. Additionally, the circular bus bars are installed into the FETs at this time; these were a custom part created to screw into the MOSFET module and carry power up to the Traction Board.

The box is designed to run at a constant pressure of 50 PSIG, via flowing the fluid with an external pump. The design is for the fluid flow to be forced underneath the MOSFET modules using a manifold, seen in Figure 13a, which is then attached to the fluid output of the box, seen in Figure 13b; the manifold pulls the fluid underneath the MOSFETs

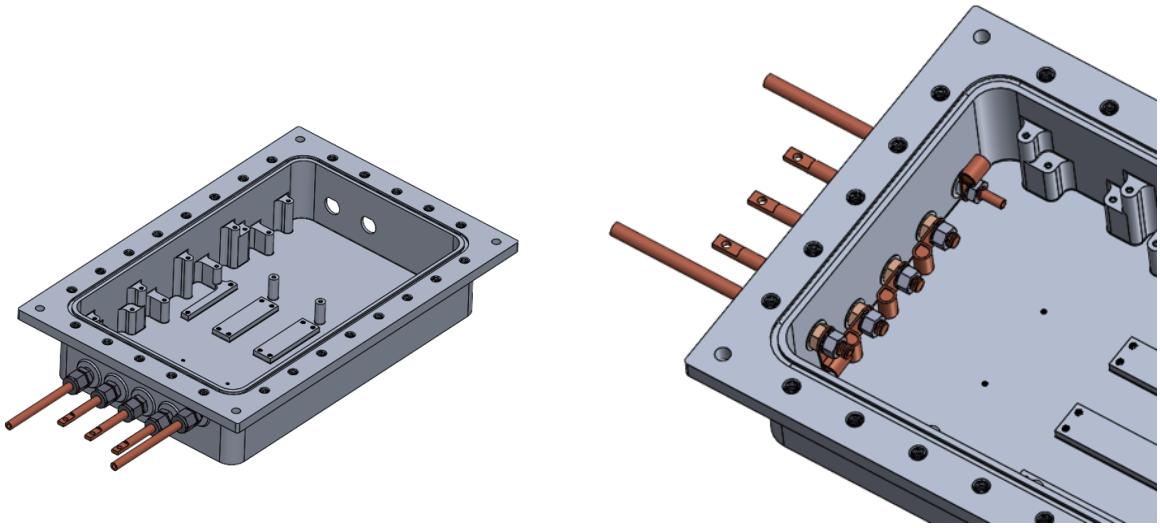

(a) Power Connectors View from Outside **(b) Power Connectors View from Inside**

Fig. 10 High Power Connectors Mounted to Enclosure

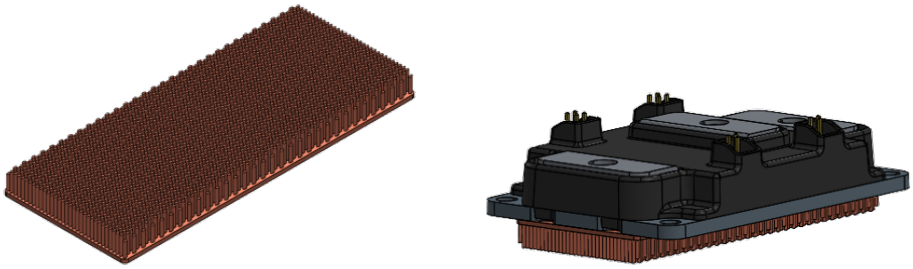

(a) Copper Elliptical Pin Fin Heat Sink **(b) MOSFET with Attached Pin Fin Heat Sink**

Fig. 11 Pin Fin Heat Sink

to cool them. The MOSFETs are the hottest part of the design, accounting for 990 - 1,140 W of loss, depending on the switching frequency, during full power operation. Many of the electronics have lower temperature limits than the MOSFETs and together produce less than 22 W of loss. Because of this, it was ideal to have the fluid pass under the FETs last, which is accomplished with this manifold design. This way, the hottest fluid is immediately pulled out of the box, rather than moving back over the sensitive electronics. There is an electrical advantage to pressurizing the box as well, in that the effects of the Paschen Curve can be avoided at flight altitudes.

D. Circuit Boards

Once the MOSFETs, manifold, and external connectors were installed, the rest of the circuit boards were installed. The Driver Board is installed directly on top of the FETs, seen in Figure 14. This was done to minimize inductance on MOSFET gate signals, as high inductance on these lines will damage MOSFETs [2]. The inductance in the line is directly proportional to the trace length, and therefore necessitates the close placement of the Driver Board and gate circuitry to the MOSFET gate pin. After the Driver Board is installed, the Controller Board is plugged in, seen in Figure 15a; there are three board-to-board connectors between these two boards. Then, the wire connections from the

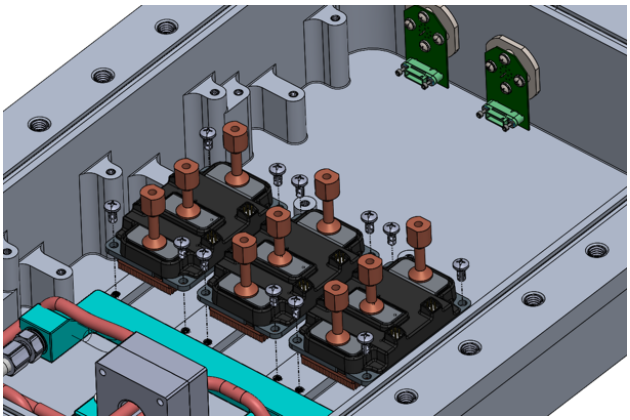

Fig. 12 MOSFETs in Enclosure

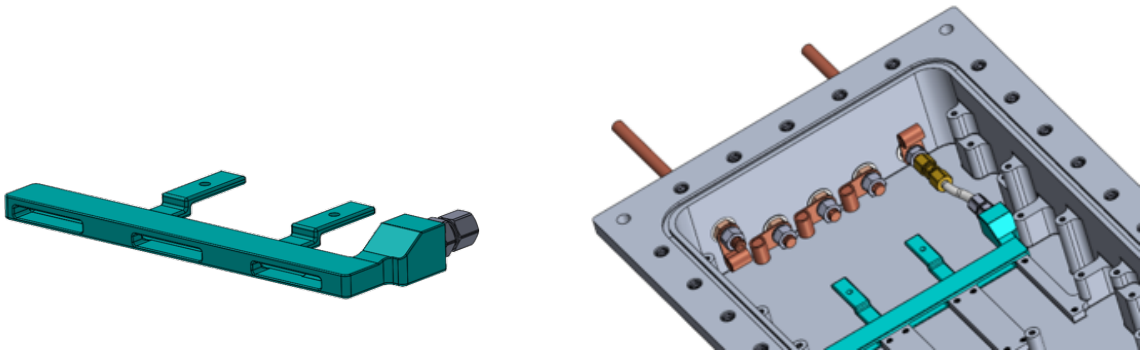

(a) Manifold **(b) Manifold in Enclosure**

Fig. 13 Manifold Design

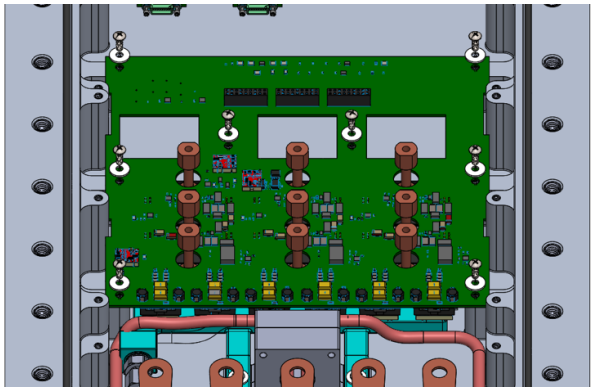

Fig. 14 Driver Board Installed in Enclosure

box hermetic connectors are plugged into the Controller. The last PCB to be installed is the Traction Board, seen in Figure 15b. The circular FET bus bars are screwed into this board, and the cable connectors are attached between this board and the Controller.

All circuit boards are mounted to fixed standoffs that were machined into the enclosure. Some of these connections are both electrical and mechanical in nature, as discussed in the electrical section. In these instances, copper washers were used to facilitate the connection. Where isolation was desired, plastic PTFE washers were used; again in this instance the material type was important, as to not react with the PAO.

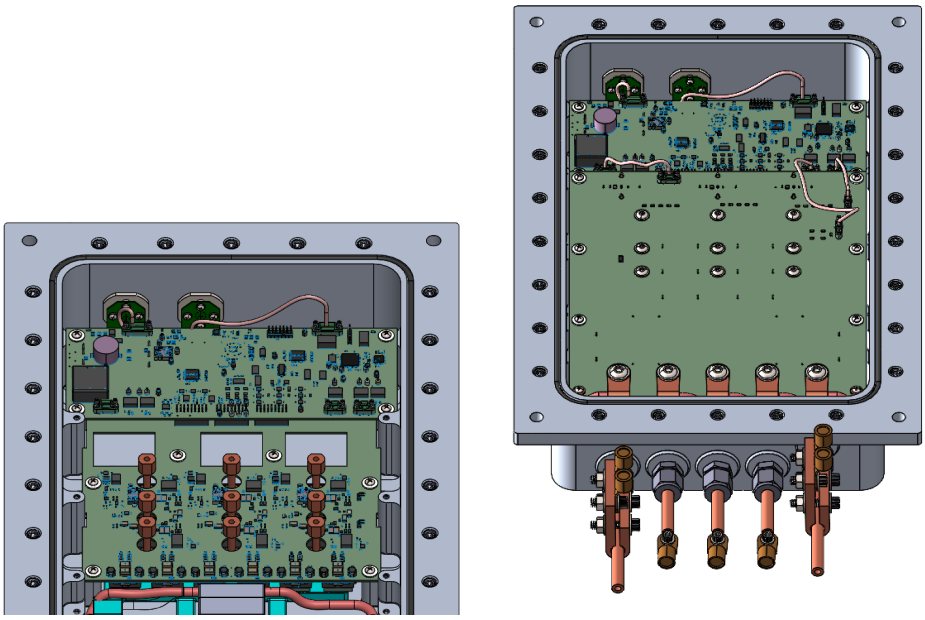

(a) Controller Board Installed in Enclosure **(b) Traction Board Installed in Enclosure**

Fig. 15 Controller and Traction Boards Installed

E. Lid and Pressure Testing

With all the PCBs and connectors installed, the o-ring sealed lid can finally be installed on the enclosure, seen in Figure 16. This lid also features mounting holes which can be used to hold an Ethernet to fiber optic converter, if there is a desire to run optical communications to the unit. This part was placed outside of the enclosure, rather than inside, because standard optical transceivers are not compatible with fluid. Readily available hermetic optical connectors could not be located within the timeline, budget, or desired level of complexity, so copper communication was used to transition from inside the enclosure to outside. The copper Ethernet cable which exits MAGIC can then be plugged directly into a computer, or plugged into the optical transceiver if desired.

To verify that the MAGIC enclosure can safely contain 50 PSIG of internal pressure, a hydrostatic test was performed. During this test, the enclosure was pressurized to a maximum of 75 PSIG. The internal pressure began at 50% pressure and held for five minutes. The pressure gradually increased by 10% increments and held for 5 minutes during each increment until 100% pressure was achieved. The final pressure was held for a total of 15 minutes. With this success, the enclosure passed pressurization testing and was ready for immersion testing.

IV. Software and GUI Design

A. Software Overview

The software and graphical user interface (GUI) used by MAGIC evolved from the X-57 HLMC software and GUI [3]. The motor control algorithm runs on the same TI C2000 chip and the code is generated from a Simulink model in the same manner as HLMC [4]. The GUI sends commands to, and receives telemetry from, the motor controller via Ethernet.

B. Motor Control

The motor controller software executes a bidirectional motor control algorithm, which is field-oriented control (FOC). The core of the algorithm relies on measuring two phase currents, calculating the third, then transforming the current measurements from AC signals in the stationary frame to DC signals in the rotating frame. Proportional-integral (PI) control is then performed using the error between the measured and commanded current, which is proportional to torque. A positive current command will convert DC bus power to AC power to electrically drive a connected motor. A

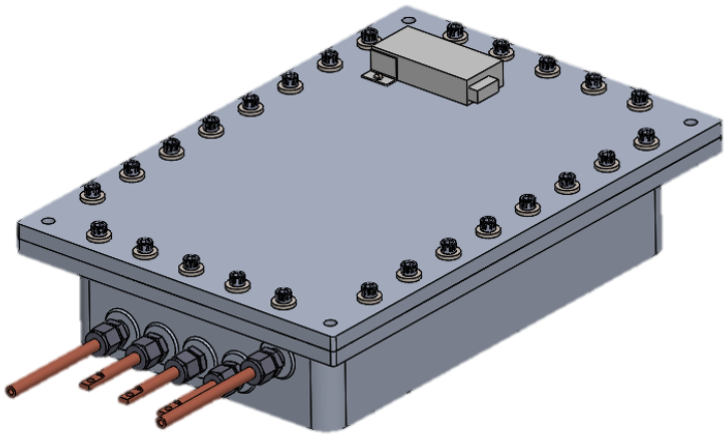

Fig. 16 MAGIC Enclosure with Lid

negative current command will convert AC power from a mechanically driven motor into DC power on the bus.

When electrically driving a connected motor, an outer speed PI control loop generates a current command for the current control loop using the error between the measured and desired speed. An outer state machine governs the speed loop to control when and how the motor spins. The motor angle and speed for transformations and control loop calculations are estimated using an observer. These values are required for both spinning a motor and power generation from a motor.

A motor start algorithm is implemented to spin up a connected motor, since angle and speed are required and observer estimates are inaccurate at low speed. Spinning up a motor involves pushing sinusoidal current of increasing frequency through the motor to spin it to a speed where the observer estimate becomes accurate [5]. In similar fashion, a synchronization algorithm is needed to begin power generation from a motor. Phase voltage sensors are used to estimate motor angle and speed, to achieve observer synchronization with a connected motor before the MOSFETs begin switching.

C. GUI

The GUI supports displaying 14 unique telemetry signals at a time and multiple display methods can be used simultaneously for each signal. There are many telemetry signals available within the motor controller software including FOC values, observer values, ADC measurements, and fault signals. More telemetry signals are available than can be displayed, so the GUI allows received signals to be swapped by the user during operation. The GUI also provides the option to record received telemetry, which is saved at the control rate of 14 kHz, to a comma-separated values (CSV) file. A sample configuration for the GUI can be seen in Figure 17.

V. Testing and Results

A. Initial Testing

After the MAGIC PCBs went through basic checkout tests they were assembled on a cold plate, seen in Figure18, to ensure they worked before covering in fluid, as the fluid adds a layer of complexity to trouble shooting. This cold plate MAGIC build completed full DC bus voltage (270 V) and full AC current (140 Arms) testing. Additionally, it has been tested with a COTS motor attached to a dynamometer and loaded to produce 10 kW. Once successful in the cold plate version, MAGIC was assembled in its enclosure for immersion testing.

B. Stagnant Immersion Testing

MAGIC was assembled in its enclosure and the Opticool-MIL 87252 fluid was added to it, covering all the electronics, see Figure19 . The lid was left off for better access during initial testing.

Fluid was first added to the enclosure on April 5th, 2024 and remained in for approximately two months. The unit

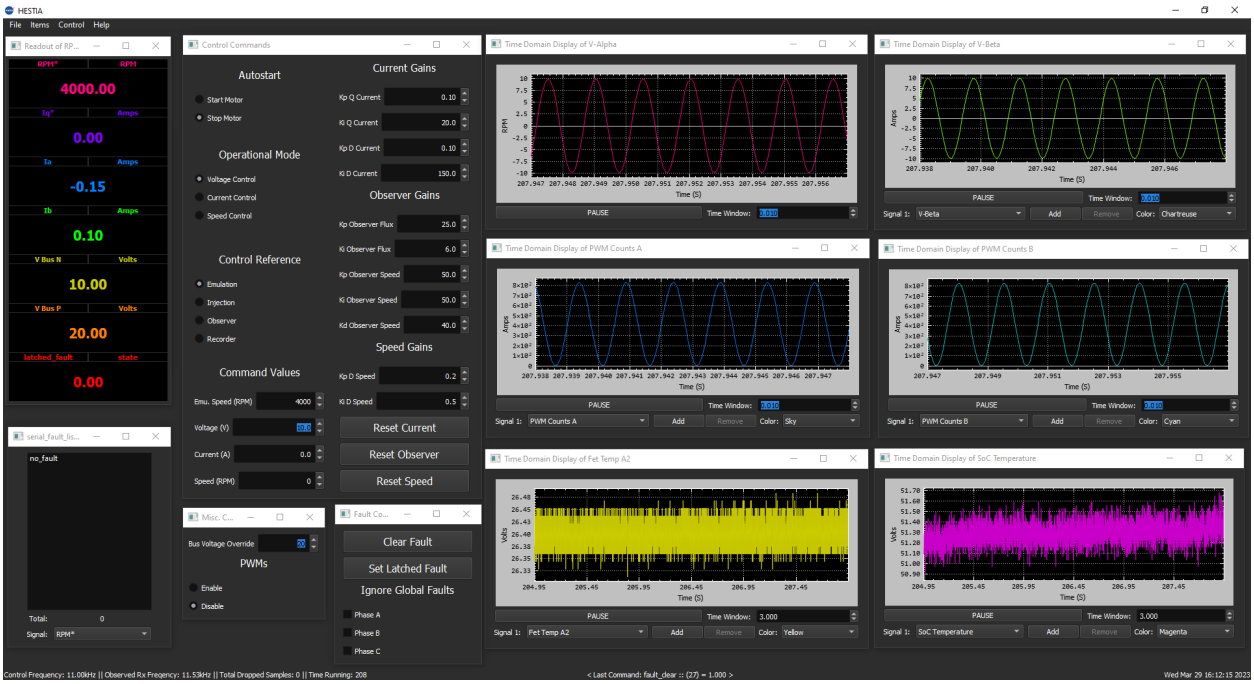

Fig. 17 MAGIC GUI screenshot

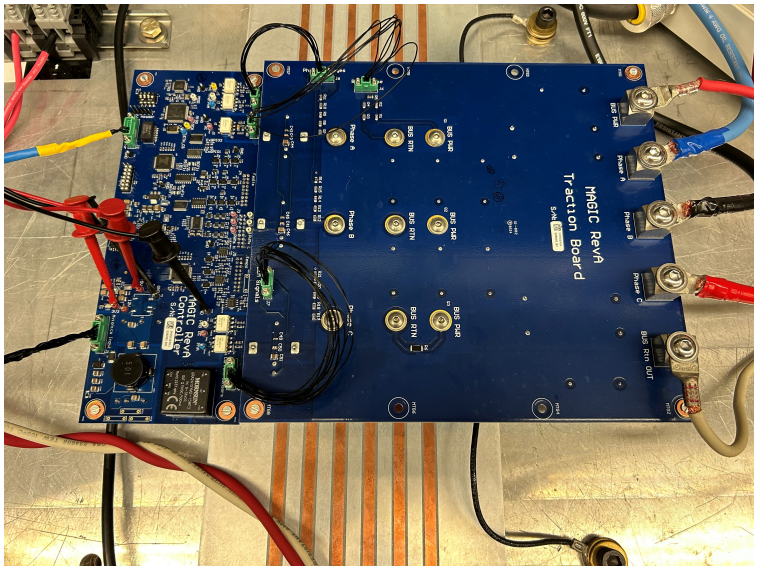

Fig. 18 MAGIC Cold Plate Setup

performed well in all testing, achieving full voltage and 10 kW operation, and was able to run with stagnant fluid without overheating. The biggest discovery from this initial immersion came when the box was first drained, upon which it was discovered that the MOSFET modules were exuding a transparent substance. It became apparent that the FETs were not completely sealed parts. This allowed the internal silicone potting material of the MOSFETs to be exposed to the PAO fluid, and silicone is incompatible with our selected dielectric fluid. This caused the potting material to expand and seep out of every opening in the MOSFET package. Despite this, there was no observed degradation in MOSFET electrical performance. It is assumed that any potting material lost in the FETs was replaced by PAO, therefore preserving the isolation requirements of the part.

After this discovery, a single MOSFET module was completely submerged in a small container of PAO. It was

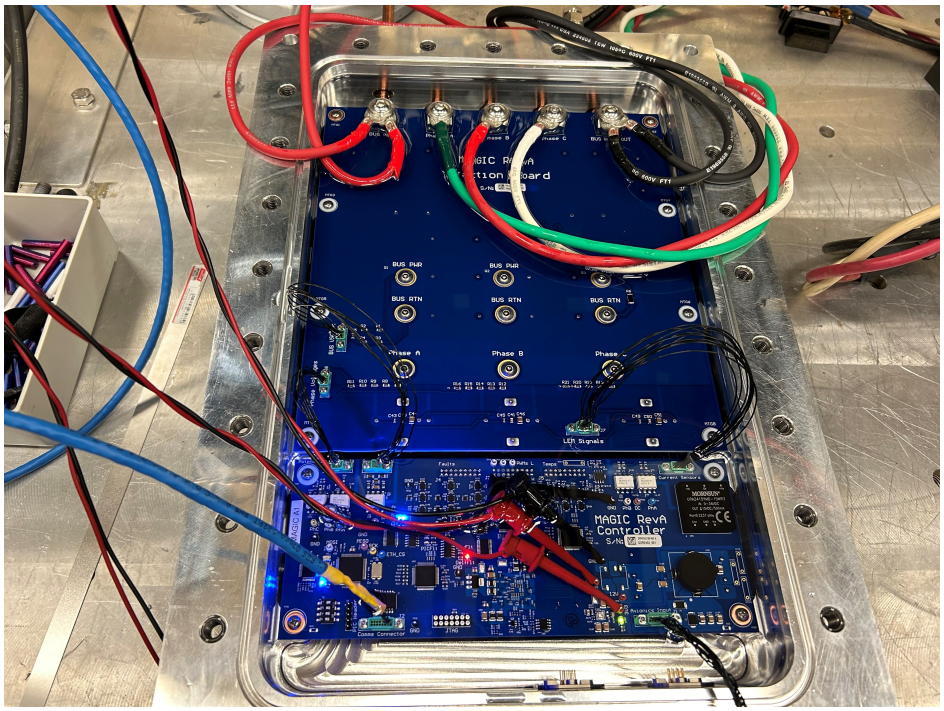

Fig. 19 MAGIC Immersion Setup - Lid Off

observed that the silicon potting material started to seep out of the FET within as little as two weeks time. This was observable by the naked eye, but it is possible this break down could have been observed earlier using a magnifying device. Despite the continued successful electrical operation of the converter using the MOSFET modules, we recommend not using unsealed modules in PAO immersion designs due to the breakdown of potting material. The material breakdown makes exact electrical parameters of the MOSFET unknown, and any loose material is free to float around in the fluid and can potentially clog pipes and filters.

C. Full Power Testing

Pump-back testing was conducted to achieve full power after functional testing and stagnant fluid testing were complete. Two MAGIC units were connected together on the AC side and DC side for this test. A power supply on the DC bus set the bus voltage and provided power to cover losses in the test setup. This configuration is possible due to MAGIC being a bi-directional converter, capable of switching AC to DC and DC to AC. This setup is advantageous in that it allows for full power testing without needing a supply or load capable of handling the full power. Magnetics are used between the AC ports to provide impedance to limit and regulate circulating currents. A diagram of the pump-back setup can be seen in Figure 20.

The main issue that was resolved to enable pump-back testing was reduction of common-mode current between the two converters. In addition to load inductance on each phase, a common mode inductor was added between the three phases to reduce common mode currents. Common mode current stemmed from imbalance between the three phases and unsynchronized switching between the two converters. Common mode current stemming from phase imbalance was mitigated through zero-sequence voltage injection. Once this was resolved, full power operation of 37.5 kW was achieved in the converter. The test was repeated several times successfully.

D. Motor Overspeed Sensor Testing

In order for the MAGIC software to remain non-safety-critical, a motor overspeed sensor was designed in hardware to sense if the motor was about to cross into an unsafe RPM region. This type of circuit design was needed because this is a sensorless motor controller that does not use an encoder which would contain this type of information.

The overspeed detection circuit fundamentally functions by sensing the back-EMF frequency of the phase voltage.

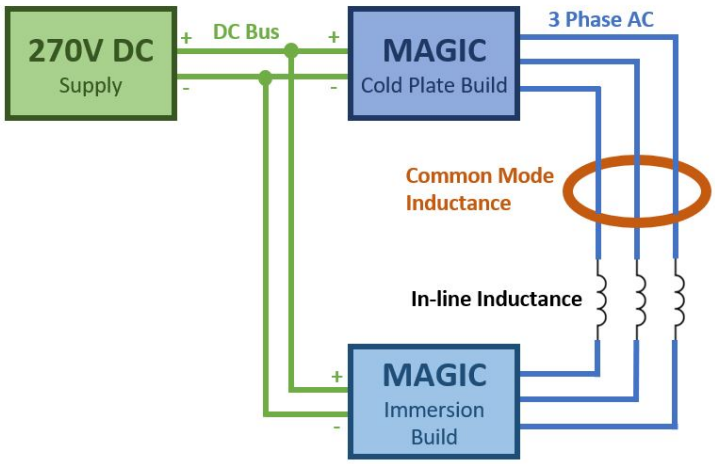

Fig. 20 MAGIC Pump Back Test Diagram

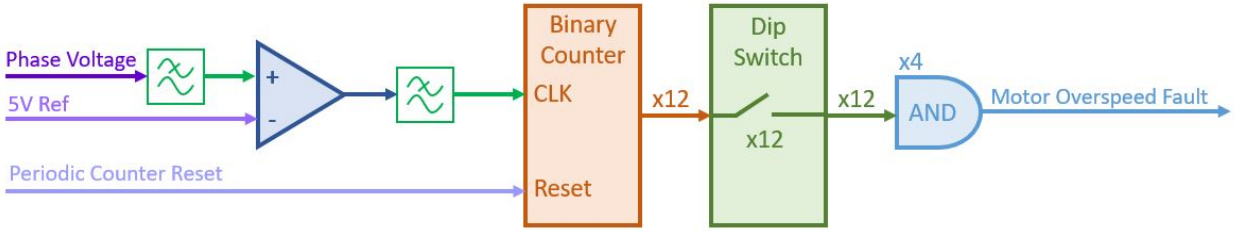

Fig. 21 Motor Overspeed Sensor Circuit

The phase voltage reading is filtered and passed through a comparator to convert it into a digital pulse train. The pulse is fed into a binary up-counter which is periodically reset. A series of logic gates monitors the output of the up-counter. A fault signal is latched if the outputs of the up-counter exceed a tunable threshold, which corresponds to a specific rotor speed. A block diagram of this circuitry can be seen in Figure 21.

A minor risk of this overspeed sensing strategy is that the phase voltage amplitude is dependent on the back-emf amplitude. If the back-emf amplitude were too low, it may fall below the hysteresis threshold of the comparator and become unobservable. This risk is mitigated by the fact that back-emf is proportional to rotor speed in electric machines, so any dangerously high rotor speed will correspond to a sufficiently strong phase voltage signal.

This circuit was built and tested. Math can be done to relate the motor speed, phase voltage, and output of the up-counter, to set the trip level to a desired motor speed. The circuit performed as expected and allows for the software to remain non-safety-critical as it is a hardware overspeed protection circuit.

VI. Conclusion

NASA GRC developed a fluid immersion cooled, SiC MOSFET, 37.5 kW, bi-directional motor converter. The positive impacts of immersion cooling are freedom from bulky metal heatsinks, no reliance on access to air flow for cooling, pressurizing the enclosure to avoid effects of the Paschen curve, potentially longer life for electronics due to constant thermal regulation, and more. The biggest lesson learned from this testing was that not all MOSFET modules are sealed and therefore should not be used with PAO, as the potting material is incompatible. In general, material compatibility is one of the biggest areas needing special attention in a system like this. The success of the pump-back test configuration and motor overspeed sensor were also noteworthy accomplishments. Future testing plans include fluid flowing thermal testing while pumping and chilling/heating the PAO fluid.

Acknowledgments

This work is sponsored by the NASA Transformative Aeronautics Concepts Program (TACP) - Convergent Aeronautics Solutions (CAS) SUb-sonic Single Aft eNgine (SUSAN) effort, along with the Advanced Air Vehicles Program (AAVP) - Advanced Air Transport Technology (AATT) - Advanced Power Electronics group, and performed at NASA's Glenn Research Center (GRC).

References

[1] "High-Power Advanced Cable Technology (hiact)," , May 2023. URL `https://www1.grc.nasa.gov/aeronautics/eap/facilities/hi-act/`.

[2] Batzel, T. D., and Leach, T. R., "Gate drive and efficiency analysis for a silicon carbide mosfet based electric motor drive," *5th IAJCISAM Int. Conf*, 2016.

[3] Kowalewski, S. R., Blystone, J., Maroli, J. M., Granger, M., Avanesian, D., Belovich, E., Liederbach, G., and Miller, W., "NASA's X-57 High Lift Motor Controller: Detailed Design, Test Results, and Outcomes," *AIAA AVIATION FORUM AND ASCEND 2024*, 2024, p. 4134.

[4] Maroli, J. M., Morris, B. A., Blystone, J. A., and Oconnor, A. M., "Utilizing Code Generation from Models for Electric Aircraft Motor Controller Flight Software," *AIAA AVIATION 2023 Forum*, 2023, p. 4274.

[5] Wang, Z., Lu, K., and Blaabjerg, F., "A simple startup strategy based on current regulation for back-EMF-based sensorless control of PMSM," *IEEE Transactions on Power Electronics*, Vol. 27, No. 8, 2012, pp. 3817–3825.